Modeling Crack Growth Processes in Fusion Reactor Materials

R.H. Jones and W.G. Wolfer

September 1983

UWFDM-553

Presented at the Third Topical Meeting on Fusion Reactor Materials, Albuquerque, NM, 19-23 September 1983.

FUSION TECHNOLOGY INSTITUTE

UNIVERSITY OF WISCONSIN

MADISON WISCONSIN

"LEGAL NOTICE"

"This work was prepared by the University of Wisconsin as an account of work sponsored by the Electric Power Research Institute, Inc. ("EPRI"). Neither EPRI, members of EPRI, the University of Wisconsin, nor any person acting on behalf of either:

"a. Makes any warranty or representation, express or implied, with respect to the accuracy, completeness, or usefulness of the information contained in this report, or that the use of any information, apparatus, method, or process disclosed in this report may not infringe privately owned rights; or

"b. Assumes any liabilities with respect to the use of, or for damages resulting from the use of, any information, apparatus, method or process disclosed in this report."

Modeling Crack Growth Processes in Fusion Reactor Materials

R.H. Jones and W.G. Wolfer

Fusion Technology Institute
University of Wisconsin
1500 Engineering Drive
Madison, WI 53706

http://fti.neep.wisc.edu

September 1983

UWFDM-553

Presented at the Third Topical Meeting on Fusion Reactor Materials, Albuquerque, NM, 19-23 September 1983.

MODELING CRACK GROWTH PROCESSES IN FUSION REACTOR MATERIALS

Russell H. Jones

Pacific Northwest Laboratory, Richland, Washington 99352

Wilhelm G. Wolfer

University of Wisconsin, Madison, Wisconsin 53706

Models for the effect of the chemical environment on crack growth processes in austenitic and ferritic stainless were evaluated. The effect of impurity segregation, yield strength, and hydrogen on crack growth of HT-9 and radiation induced phosphorus segregation on the intergranular stress corrosion of 316SS have been evaluated. Moderate increases in impurity segregation and/or yield strength caused significant decreases in the K_{IC} and K_{TH} of HT-9, while less than a 10 fold increase in the intergranular stress corrosion crack growth rate of 316SS was predicted for a fluence of 100 dpa using the radiation induced phosphorus segregation data of Brimhall et al. and the stress corrosion model of Parkins. Therefore, while radiation induced impurity segregation is greater in 316SS than HT-9, the effect of impurity segregation may be more pronounced in HT-9. The effect of hydrogen on fatigue crack thresholds was evaluated using a model by Tien which describes the threshold as a function of surface energy. A reduction in the surface energy by hydrogen adsorption was found to cause a decrease in the fatigue threshold a small but comparable amount to that observed for 2-1/4Cr-1Mo steel.

1. INTRODUCTION

Fracture in fusion reactor structural materials may occur by rapid unstable flaw growth or slow sub-critical flaw growth. The lifetime of fusion reactor structural materials, and hence fusion reactors, will be a function of many factors such as load, temperature, neutron irradiation and plasma-wall and coolant-material interactions. Neutron induced embrittlement may decrease the stress needed for unstable flaw growth because of irradiation hardening, irradiation induced precipitation, segregation, and helium generation, while cyclic stresses and temperatures may cause flaws to grow to a size which propagate in an unstable, rapid manner.

Sub-critical flaw growth can occur by a variety of processes such as fatigue, stress corrosion, corrosion fatigue, hydrogen embrittlement and creep crack growth. Sub-critical flaws may grow to a size which allowscoolant leakage into the plasma chamber or tritium escape into the blanket or containment building or to a critical flaw size which propagates very rapidly. Sub-critical crack growth rates are a function of material parameters such as microstructure, chemistry, segregation, environment chemistry, and loading parameters. Fracture morphology may be transgranular, intergranular, or mixed depending on material condition, environment, and loading.

Since the structural integrity of a fusion reactor is a critical design criterionand because the complexity of radiation and environmental effects on fracture processes will preclude obtaining experimental results for all environment combinations, models describing these interactions can be used to enhance a limited data base.

2. INTERGRANULAR FRACTURE OF HT-9

2.1 Unstable Flaw Growth

Segregation of impurities such as phosphorus, sulfur, antimony and tin are known to affect the fracture toughness and crack growth of ferritic

steels at low and elevated temperatures.[1-3] In austenitic stainless steels segregation may alter the time dependent crack growth processes at elevated temperatures[4] but segregation does not have a large effect on time independent fracture processes. Also, segregation may occur in fusion reactor materials during heat treatment, fabrication and service. Brimhall, Baer and Jones[5] have shown that radiation greatly enhances the segregation of phosphorus in 316SS and causes a modest enhancement of phosphorus segregation in HT-9. Therefore, it is important to evaluate the effect of impurity segregation on intergranular fracture.

Recently Gerberich and Wright[6] presented a model for the effect of impurity segregation on the intergranular K_{IC} of a ferritic steel using the intergranular fracture stress versus grain boundary segregation data of Kameda and McMahon[1] as a basis for their model. Gerberich and Wright noted that Kameda and McMahon's data could be represented by the following expression:

$$\sigma_f^* = \sigma_{f_o}^* - \alpha_i^* \bar{X}_i^{1/2} \qquad (1)$$

with $\sigma_{f_o}^*$ defined as the fracture stress in the absence of segregant, $\bar{X}_i$ being the average grain boundary concentration and α_i^* a coefficient which describes the embrittling potency of a segregated impurity. Values of α_i^* were 3100 MPa (at. fract.)$^{-1/2}$ for antimony and 1200 MPa (at. fract.)$^{-1/2}$ for phosphorus. Using a model which considers the stress tensor in the plastic region at the tip of a blunt crack, relationships for the distance from the crack tip to the maximum stress, crack tip radius and the plastic constraint factor as a function of K_I were derived. Assuming that $K_{IC} = K_I$ at $\sigma_{yy}^{max} = \sigma_f^*$ the following model for the fracture toughness was derived:

$$K_{IC} = \frac{E\rho_o}{\alpha'}\left\{\exp\left[\frac{\sigma_{f_o}^* - \alpha_i^* \bar{X}^{1/2}}{\alpha'' \sigma_y} - 1\right] - 1\right\} \qquad (2)$$

where $\rho = \rho_o (\sigma_y/K_I)$, ρ = crack tip radius, $r = \alpha' K_I^2/\sigma_y E$, r = distance to maximum stress, E = elastic modulus, $\sigma_{f_o}^*$ = intergranular fracture stress without segregant, α_i^* = embrittling effectiveness of impurity, $\bar{X}_i$ = average grain boundary concentration of impurity, α'' = strain hardening factor, σ_y = yield strength. With the following values assumed for the parameters in Equation 2: $\alpha'' = 1$, $\alpha' = 2$, $E\rho_o = 45.5$ MPa $\sqrt{m}$, $\sigma_{f_o}^* = 2750$ MPa, $\sigma_y = 840$ MPa, and the values for α_i^* given previously, good agreement was obtained between Equation 2 and the results of Kameda and McMahon.[1]

Application of Equation 2 to HT-9 requires data for several parameters including grain boundary chemistry. Comparison with experiment requires K_{IC} data in which integranular fracture predominates. However, present experimental data[7-9] does not indicate that heat treatment or irradiation to 10^{22} n/cm^2 at 423°C causes intergranular fracture in HT-9. The purpose for evaluating Gerberich and Wrights intergranular K_{IC} model, therefore, is to help assess whether intergranular fracture is likely under fusion reactor conditions and as a step to evaluating the effect of segregation and hydrogen on subcritical crack growth.

Jones and Thomas[7] recently evaluated the effect of heat treatment on the grain boundary chemistry and charpy impact fracture of HT-9. The microstructure, tensile properties and subcritical crack growth were also evaluated so that there is sufficient data to evaluate K_{IC} using Equation 2 and K_{TH} using the analysis presented in the next section. Pertinent property data for HT-9 evaluated by Jones and Thomas[7] are presented in Table I. Since the steel evaluated by Gerberich and Wright[6] had a comparable microstructure and yield strength to HT-9, the strain

hardening factor, α'', the location of the maximum stress ahead of the crack tip, $r \alpha \alpha'$, and the crack tip radius coefficient, ρ_o, would also be similar. However, sulfur segregation was observed in HT-9 and the value of α_i^* for sulfur has not been previously reported. Jones et al.[10] found that antimony was equally or more effective than sulfur in causing intergranular fracture of iron; therefore, it is reasonable to assume, for this analysis, that sulfur and antimony have equal embrittling effectiveness in ferritic steels.

The value for $\sigma_{f_o}^*$ is more difficult to estimate for HT-9 than are the other input parameters. Gerberich and Wright[6] estimated a value of 2750 MPa for the 3.5 NiCrMoV steel evaluated by Kameda and McMahon[1] by extrapolating the σ_f^* results to zero impurity concentration. However, this stress is a function of microstructural features such as prior austenite grain size and grain boundary carbide size and spacing. Since the microstructural data for the 3.5 NiCrMoV steel is unknown, a value for $\sigma_{f_o}^*$ for HT-9 has been obtained by evaluating Equation 2 for a known K_{IC} and grain boundary segregation. A value for the K_{IC} of HT-9 can be obtained from the charpy impact results in Table I and the relationship by Barsom and Rolfe,[9] Equation 3:

$$\left(K_{IC}/\sigma_y\right)^2 = \frac{5}{\sigma_y}\,(CVN - \sigma_y/20). \qquad (3)$$

Using the upper shelf fracture energies given in Table I, Equation 3 gives K_{IC} values of 160 and 155 MPa $\sqrt{m}$ for heat treatments 1 and 2, respectively. With the grain boundary chemistries listed in Table I and the values for α', α'', ρ_o, and α_i^* discussed previously, values of $\sigma_{f_o}^*$ of 2237 MPa and 2413 MPa are obtained. The charpy fractures were transgranular and not intergranular, therefore, the intergranular K_{IC} must exceed 155 MPa $\sqrt{m}$ and so $\sigma_{f_o}^*$ must exceed 2413 MPa. Since the yield strength of HT-9 is less than the 3.5 NiCrMoV steel evaluated by Kameda and McMahon[1], the microstructure is probably on a coarser scale. Therefore, it is expected that the $\sigma_{f_o}^*$ for HT-9 is less than 2750 MPa but greater than 2413 MPa. A value of 2500 MPa was assumed for $\sigma_{f_o}^*$ which gives a calculated intergranular K_{IC} for HT-9 of 273 MPa $\sqrt{m}$ and 360 MPa $\sqrt{m}$ for heat treatments 1 and 2. These results indicate the sensitivity of Equation 2 to small changes in $\bar{X}_i$ and σ_y and hence any irradiation enhanced impurity segregation or hardening is of concern in ferritic materials. This sensitivity is demonstrated by the calculated K_{IC} values for HT-9 given in Figure 1. The detrimental effect of both segregation and yield strength increasing simultaneously is clearly shown. Also, modest yield strength or segregation increases decrease K_{IC} significantly. For instance, K_{IC} is decreased from 273 MPa $\sqrt{m}$ to 100 MPa $\sqrt{m}$ by either an increase in $\bar{X}p$ to 0.25 monolayers or an increase in σ_y to about 680 MPa. Combined values of $\bar{X}p = 0.1$ and $\sigma_y = 600$ MPa are sufficient to decrease K_{IC} to 100 MPa $\sqrt{m}$. Fracture toughness values of less than 40 MPa $\sqrt{m}$ may occur with $\bar{X}p = 0.6$ or σ_y = 1100 MPa or both. Irradiation can cause

TABLE I. Grain Boundary Chemistry, Microstructure and Mechanical Property Data for HT-9

Heat Treatment	Grain Chemistry P	Boundary Monolayers S	Microstructure Data: Prior γ	Lath Size	Sub-Grains	Mechanical Properties: 0.2 YS MPa	UTS MPa	ε_u	ε_f	Upper Shelf Impact, J
760°C/2.5h	0.015	0.03	100 μm	15 μm	1 μm	510	780	0.13	0.21	81
760°C/2.5h 540°C/240h	0.04	0.01	100 μm	15 μm	1 μm	510	780	0.096	0.17	77

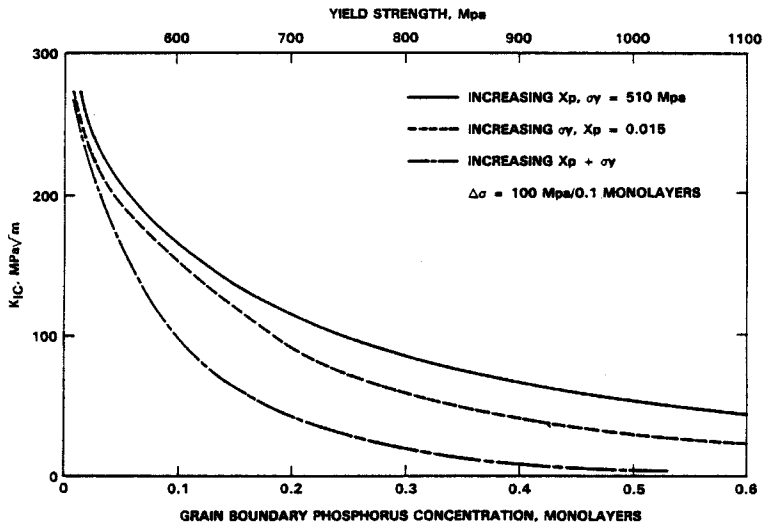

FIGURE 1
Calculated fracture toughness of HT-9 with varying grain boundary phosphorus concentration and yield strength.

nonequilibrium segregation with grain boundary concentrations exceeding the equilibrium limits and irradiation of HT-9 to high fluences may also produce higher yield strengths. Therefore it appears that intergranular fracture of HT-9 in fusion environments is a possibility.

2.2. Intergranular Fracture Threshold of HT-9 in Hydrogen

It has been shown by Jones and Thomas[7] and Hyzak and Garrison[11] that HT-9 is susceptible to intergranular fracture in the presence of hydrogen. In both cases impurity segregation and hydrogen were co-embrittlers as has been suggested for several ferritic steels.[1,12-15] Therefore, analysis of combined impurity and hydrogen effects on ferritic steels is important to fusion reactor materials development.

Gerberich and Wright[6] used the data of Kameda and McMahon to model the combined effect of impurities and hydrogen on the sub-critical crack growth threshold, K_{TH}. They used Briant et al's.[16] concept for the additive effect of impurities and hydrogen, a relationship for the effect of hydrogen on σ_f^* observed for a Ti-5 Al -4Mo alloy and an expression for the hydrogen concentration given by Li[17] to derive Equation 4, where: σ_H^* = embrittling effectiveness of hydrogen, C_o = initial concentration of hydrogen, and $\bar{V}_H$ = partial molar volume of hydrogen.

Using the input parameters for HT-9 given in the previous section and 120 MPa for $\alpha_H^* C_o^{1/2}$, 2J/mol-MPa for $\bar{V}_H$ as per Gerberich and Wright[6] and the grain boundary chemistry and yield strength data for HT-9 listed in Table I, sub-critical crack growth thresholds of 174 MPa $\sqrt{m}$ and 225 MPa $\sqrt{m}$ for heat treatments 1 and 2 respectively, were obtained by numerically solving Equation 4. These K_{TH} values are 0.64 and 0.63 of the calculated intergranular K_{IC} values for HT-9 and suggest that HT-9 is susceptible to

$$\sigma_{f_o}^* - \alpha_i^* \bar{X}_i^{1/2} - \alpha_H^* C_o^{1/2} \exp\left\{\frac{\alpha'' \bar{V}_H \sigma_y}{2RT}\left[1/2 + \ln\left(1 + \frac{\alpha' K_{TH}}{E p_o}\right)\right]\right\} = \alpha'' \sigma_y \left[1 + \ln\left(1 + \frac{\alpha' K_{TH}}{E p_o}\right)\right] \quad (4)$$

combined impurity and hydrogen effects. A more complete analysis of the effects of increasing $\bar{X}p$ and σ_y on K_{TH} is given in Figure 2. It can be seen that the trends are very similar to the intergranular K_{IC} values given in Figure 1 where combined increases of σ_y and $\bar{X}p$ are the most severe with K_{TH} approaching zero at σ_y = 1000 MPa and $\bar{X}p$ = 0.5 monolayers. The sub-critical fracture threshold of HT-9 in hydrogen can be decreased from 172 MPa $\sqrt{m}$ for σ_y = 510 MPa and $\bar{X}p$ = 0.015 to 50 MPa $\sqrt{m}$ for $\bar{X}p$ = 0.12 and σ_y = 625 MPa. These results clearly indicate the potential for intergranular sub-critical crack growth of HT-9 when irradiation induced hardening or segregation occurs.

A graphic illustration of the effect of increasing $\bar{X}p$ and σ_y on intergranular fracture of HT-9 is given in Figure 3. The da/dt versus K curves are only schematic since the crack growth rates are not known; however, this figure shows the calculated shift in K_{IC} and K_{TH} and the approximate shape of the sub-critical crack growth rate curves for increasing values of $\bar{X}p$ and σ_y. The Stage II crack growth regime becomes less distinct with increasing $\bar{X}p$ or σ_y such that at $\bar{X}p$ = 0.6 or σ_y = 1000 MPa the stage II regime is non-existent. In this condition a very small change in the length of a sub-critical crack or in the applied stress will cause a sub-critical crack to become a critical crack resulting in rapid failure.

3. EFFECT OF PHOSPHORUS SEGREGATION ON THE INTERGRANULAR STRESS CORROSION OF 316SS

Numerous qualitative stress corrosion cracking mechanisms have been proposed to explain various aspects of stress corrosion while few analytical expressions for the stress corrosion crack growth rate as a function of the stress, stress intensity, material condition and environment have been proposed. Stress corrosion crack modeling efforts have generally taken one of two similar approaches:

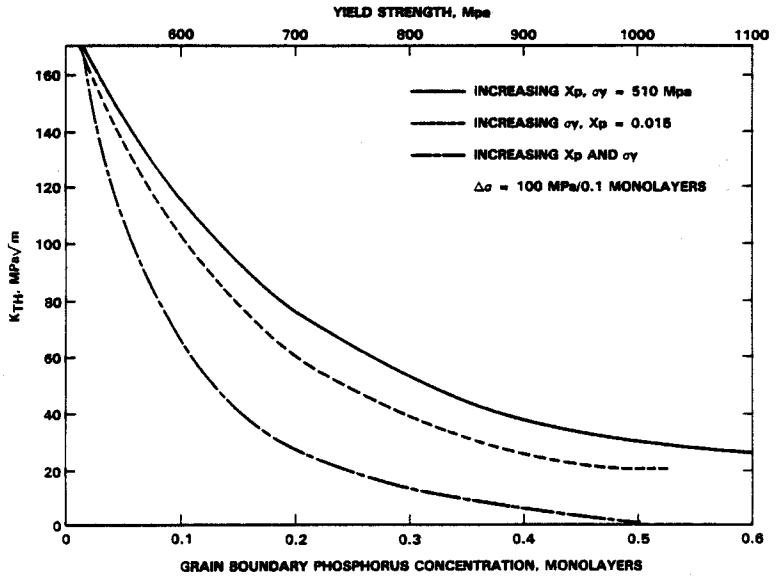

FIGURE 2
Calculated sub-critical fracture threshold, K_{TH}, of HT-9 with varying grain boundary phosphorus concentration and yield strength.

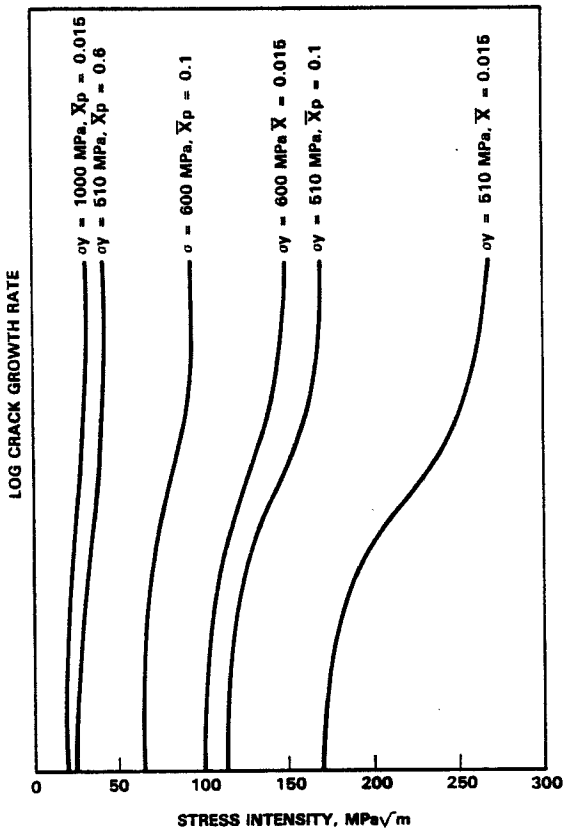

FIGURE 3
Schematic crack growth rate versus stress intensity curves for HT-9 based on calculated K_{IC} and K_{TH} values.

- Crack tip strain causes rupture of the protective film which allows active dissolution as proposed by Ford[18] and Vermilyea.[19] In this model the crack growth rate is a function of the ratio between the film rupture and repassivation rates.

- Crack growth rates are directly proportional to the anodic dissolution rate. Stress corrosion cracking occurs in many systems where protective films are stable but if the film ruptures repassivation does not occur and bare surface dissolution is thermodynamically possible as proposed by Parkins.[20] Parkin's model predicts the maximum crack growth rate for the film rupture model for the case where repassivation does not occur.

The model by Parkins has been found to fit a wide range of material environment combinations such as ferritic and austenitic steels, Aℓ - 7Mg, and brass. A common aspect of these materials for the environments in which they were examined is that they do not form very stable passive films; therefore disruption of a protective film at a crack tip will allow bare metal to occur at the crack tip while the sides of the crack are protected. In systems which form stable passive films, the balance between film rupture rate and repassivation rate dominates the crack growth rate as proposed by Ford.[18] In both cases; however, crack advance is by metal dissolution which can be described by Faraday's Law. Parkins[20] expressed the crack propagation rate as follows:

$$\frac{da}{dt} = i_a \frac{M}{zF\rho} \qquad (5a)$$

where i_a = anodic current density, M = atomic weight, z = valence, F = Faradays constant, ρ = material density.

The model by Ford[18] is very similar to Equation 5a except that i_a is replaced by Q_f/t_f where Q_f is the oxidation charge density passed in time t_f following the rupture of the protective oxide and t_f is the time between oxide rupture events. Therefore the model by Ford is expressed as follows:

$$\frac{da}{dt} = \frac{M}{zF\rho} \frac{Q_f}{t_f} \qquad (5b)$$

The crack growth rate predicted by Equation 5b is generally less than that predicted by Equation 5a because the value Q_f/t_f approaches Q/s, the bare surface current density, i_a, as $t_f \to o$.

The most common cause of intergranular stress corrosion cracking (IGSCC) in austenitic stainless steels is chromium depletion adjacent to the grain boundaries because of chromium carbide precipitation at grain boundaries; however, there is sufficient experience and understanding from the light water reactor industry of this phenomenon that it should not be a problem for

austenitic stainless steels in water cooled fusion reactors. However, a second and less studied cause of IGSCC, is that of impurity segregation (phosphorus, sulfur, etc.) to grain boundaries. In most applications impurity segregation occurs during fabrication and only moderately during service; however, Brimhall, Baer and Jones[5] have shown that irradiation can greatly enhance the segregation of phosphorus in austenitic steels and nickel based alloys. Also, there is evidence that phosphorus enhances the intergranular corrosion and stress corrosion of austenitic steel[21], nickel[22,23] and nickel based alloys.[24] Marcus, Oudar and Olefjord[25] have shown that sulfur enrichment at the surface of nickel can completely eliminate passive film formation and it has also been shown[23] that phosphorus behaves similarly. A significant difference between sulfur and phosphorus, however, is in their behavior on the surface of an anode. Phosphorus is oxidized and dissolved in the electrolyte while sulfur remains on the anode surface. Therefore, an intergranular crack propagating along a phosphorus enriched grain boundary would have a very active crack tip and relatively inactive crack walls. This situation fits very well the conditions presented in the Parkins stress corrosion cracking model and therefore is a good candidate for modeling IGSCC in a fusion reactor material.

The approach used in this evaluation is as follows:

- The grain boundary phosphorus concentration versus fluence relationship was estimated from the surface segregation versus heavy ion fluence results of Brimhall et al.[5]

$$C_p = 14.6 \log \frac{\phi t}{\phi t_o}, \% \qquad (6)$$

$$\phi t_o = 0.004$$

- The current density, i_a, versus phosphorus concentration (Equation 7) was determined from bulk 304SS+P results by Gulyaev and Chulkova.[26] These results were obtained using a standard Huey corrosion test in a solution of 0.5N HNO_3 + 22 gℓ^{-1} $K_2Cr_2O_7$. While this environment is more aggressive than the service environment, this test is used to evaluate the worst conditions which may occur in a crevice or a crack.

$$i_a = 2 + 0.5\ C_p, \frac{mA}{cm^2} \qquad (7)$$

- Substitution of Equation 6 in Equation 7 gives the following expression for the current density versus fluence

$$i_a = 2.0 + 7.3 \log \frac{\phi t}{\phi t_o} \qquad (8)$$

- Combining Equation 8 with the pertinent material parameters for 316SS in Equation 5a gives the following expression for the crack growth rate as a function of fluence:

$$\frac{da}{dt} = 4.4 \times 10^{-7} + 16.1 \times 10^{-7} \log \frac{\phi t}{\phi t_o}, \frac{mm}{s} \qquad (9)$$

Equation 9 predicts crack growth rates of 10^{-6} mm/s at a fluence of 0.01 dpa and 7.5 x 10^{-6} mm/s at 100 dpa as shown in Figure 4. These results indicate that this phenomenon is significant since a crack growing at a rate of 7.5 x 10^{-6} mm/s will propagate 1 mm in 36 h. Therefore, it is important to verify if Equation 5a is valid for 316SS and if so what measures can be taken to reduce this effect. Verification of Equation 5a for 316SS can be accomplished with stress corrosion tests on 316SS which has been thermally heat treated to produce phosphorus segregation. These tests should be conducted in a fusion reactor relevant water environment at ~300°C.

4. EFFECT OF HYDROGEN ON THE THRESHOLD STRESS INTENSITY FOR FATIGUE CRACK GROWTH

4.1. Environmental effects on fatigue crack growth

The influence of gaseous and liquid environments on fatigue crack growth is well established though incompletely understood. Wei and

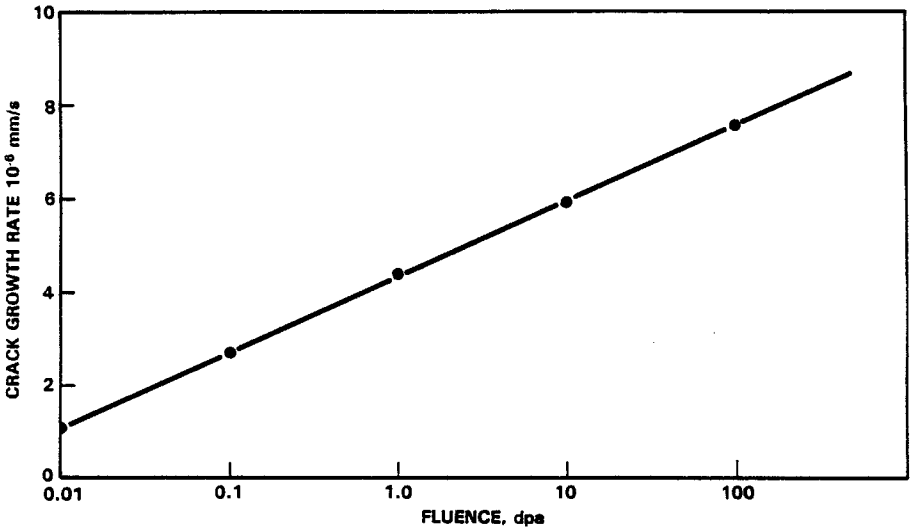

FIGURE 4
Calculated crack growth rate versus fluence for intergranular stress corrosion cracking of 316SS induced by radiation enhanced grain boundary phosphorus segregation.

Simmons[27] have investigated the effect of water vapor pressure on the rate of fatigue crack growth at room temperature for aluminum alloys, AISI 4340 steel, and 2-1/4Cr-1Mo. With increasing vapor pressure, the fatigue crack growth rate first increases until a saturation is reached at a vapor pressure which depends on the fatigue frequency and, presumably, also on temperature. The effect is thought to be controlled by the reaction of water vapor with the freshly exposed metal surface resulting in the formation of oxide and the production of hydrogen. The latter is believed to cause the acceleration of the fatigue crack growth rate. However, the rate controlling step in this acceleration is either the transport of vapor to the crack tip or the rate of chemical reaction at the crack tip. At sufficiently high vapor pressure neither of these processes becomes rate limiting, and the maximum crack growth enhancement is attained.

It is important to note that the experiments analyzed by Wei and Simmons are for fatigue crack growth in Stage II, i.e. for $da/dN \gtrsim 10^{-4}$ mm/cycle, and they do not address the question of environmental effects on the threshold for fatigue crack growth. For fusion reactor first walls in tokamaks, it is Stage I fatigue crack growth which is of particular importance to the lifetime.

In this regime, experiments have been carried out by Ritchie and coworkers[28] and others.[29-31] The results point towards two competing effects, namely the effect of hydrogen on the oxide layer and on embrittlement. For example, Tu and Seth[32] found that steam at 260°C increases the threshold of 403SS as compared to air. In contrast, Ritchie and coworkers[28] find that a dry hydrogen environment of 138 kPa pressure reduces the threshold at room temperature in 2-1/4Cr-1Mo steel when compared to the threshold in moist air. These apparently contradictory results can be rationalized by the effect of the oxide layer on fatigue crack closure. The presence of an oxide layer at the crack tip leads to crack closure; to open it and induce further

propagation requires a larger cyclic stress intensity value ΔK. Hence the promotion of an oxide layer can enhance the fatigue threshold but increase the fatigue crack growth rate in Stage II where crack closure plays a less significant role and where the oxide layer can not build up to thicknesses of the order of the crack opening displacement. The effect of a dry hydrogen environment is to eliminate the oxide layer, and thereby reduce the crack closure. When fatigue thresholds of 2-1/4Cr-1Mo tested in dry hydrogen and dry argon are compared[28] it is found that the reduction relative to moist air is mainly due to the absence of an oxide layer. Nevertheless, a small but noticeable reduction is caused by the hydrogen environment.

All these experiments address the effect of external molecular hydrogen and not internal atomic hydrogen as produced by (n,p) reactions and by permeation. In order to assess the potential effect of internal hydrogen on the threshold for fatigue crack growth it is first necessary to review the mechanism of Stage I fatigue crack growth.[33-35]

The partial crack closure formed by reversed plastic deformation in the first cycle requires that the applied load produce a stress intensity $K > K_{cl}$ to open up the crack again. Hence, the effective cyclic stress intensity ΔK_{eff} which drives crack propagation is

$$\Delta K_{eff} = \begin{cases} K_{max} - K_{cl} = \frac{\Delta K}{1-R} - K_{cl} & \text{for } K_{min} < K_{cl} \\ K_{max} - K_{min} = \Delta K & \text{for } K_{min} > K_{cl} \end{cases}$$

where $R = K_{min}/K_{max}$ and ΔK is the applied cyclic stress intensity. The minimum or threshold value of ΔK, denoted by ΔK_o, below which crack propagation no longer occurs is then

$$\Delta K_o = \begin{cases} (1-R)\ (\Delta K^o_{eff} + K_{cl}) & \text{for } K_{min} < K_{cl} \\ \Delta K^o_{eff} & \text{for } K_{min} > K_{cl} \end{cases} \quad (10)$$

Based on energy considerations[33,35] the following expression can be derived for the critical threshold value

$$\Delta K^o_{eff} = \left[\frac{4\pi E\ \gamma}{2 - (\sigma_u \varepsilon_f / \sigma_y)/(1+n)} \right]^{1/2} \quad (11)$$

Here, E is the Young's modulus, γ the surface energy, n the cyclic strain hardening exponent, σ_u is the ultimate stress and σ_y is the yield stress. Crack advance is assumed to occur when the strain ahead of the crack tip reaches the fracture strain ε_f.

Hydrogen may affect ΔK_o in two distinct ways. First, as mentioned before, it can remove the oxide layer at the crack tip and thereby reduce K_{cl}. For R-ratios below the critical value $R_c = K_{cl}/K_{max}$, ΔK_o is then lowered whereas no reduction should occur for $R > R_c$. This agrees with the observations of Suresh et al.[36] on fatigue thresholds for 2-1/4Cr-1Mo steel tested in moist air and dry hydrogen. Whereas hydrogen reduced the threshold relative to air for a R-ratio of 0.05, it did not for a R-ratio of 0.75.

The second potential effect of hydrogen is to reduce the surface energy γ as a result of chemisorption. This effect is present at all R-ratios and also for other surface-active gases such as oxygen. In the latter case, however, it is masked by the crack closure effect of the oxide layer at small R-ratios.

The third possibility of hydrogen affecting ΔK^o_{eff} could arise if the factor $(\sigma_u \varepsilon_f/\sigma_y)/(1+n)$ is changed. However, for medium and high-strength alloys, this factor plays a minor role in determining the value of ΔK^o_{eff}, so that any change will have little effect on ΔK_o.

4.2. Chemisorption of and reduction in surface energy by hydrogen

The heat of chemisorption of hydrogen is more exothermic than the heat of solution for all metals. As a result, the amount of hydrogen chemisorbed per exposed metal atom is much greater than the atomic fraction of hydrogen in solution whenever thermal equilibrium can be established between the surface and the bulk. Given the extreme mobility of hydrogen in most metals at elevated temperatures, thermal equilibrium is established at rates far in excess of fatigue crack growth rates. Hence, it is reasonable to assume that internal hydrogen will cover a fracture as fast as it can expand. The degree of coverage θ of the fracture surface by hydrogen is then given by the Langmuir-McLean isotherm

$$\frac{\theta}{1-\theta} = X \exp\{(G_B - G_S)/kT\} \qquad (12)$$

where X is the fraction of interstitial sites occupied by hydrogen, G_B and G_S are the Gibbs free energies for hydrogen in the bulk and on the surface, respectively, relative to a single hydrogen atom in vacuum. If E_D is the binding energy of the two hydrogen atoms in the molecule, and H_u and H_{cs} the heat of solution and chemisorption for molecular hydrogen, respectively, then $G_B \cong (H_u + E_D)/2$ and $G_S \cong (H_{cs} + E_D)/2$ when entropy terms are neglected. E_D = -432 kJ/mole, whereas G_B^{Fe} = -177.2 kJ/mole for α-Fe[37] and G_B^{Ni} = -180.5 kJ/mole for Ni.[38] The atomic heats of chemisorption are[39] G_S^{Fe} = -268 kJ/mole for α-Fe and G_S^{Ni} = -264 kJ/mole for Ni.

According to Bernard and Lupis[40], the surface energy γ is determined by

$$\gamma = \gamma_o + \frac{kT}{A} \ln (1-\theta) \qquad (13)$$

where γ_o is the energy of the clean metal surface (θ=0) and A is the area effectively occupied by a chemisorbed hydrogen atom. We shall assume that $A = a_o^2$ for bcc and $A = a_o^2/2$ for fcc metals, where a_o is the lattice parameter. In both equations 12 and 13 any interaction between hydrogen atoms on adjacent surface sites has been neglected.

The evaluation of the surface energy reduction ($\gamma - \gamma_o$) for different temperatures and internal hydrogen concentrations gives the results shown in Figure 5 for α-Fe, while the results for Ni were calculated and found to be similar to α-Fe. It is seen that even minor hydrogen levels of the order of 10 appm can lead to a significant reduction in the surface energy. Near a crack tip, the tensile hydrostatic stress during the positive stress cycle gives rise to a significant enhancement of the dissolved hydrogen above the average level in the bulk. As shown by Hirth and Carnahan,[41] the local concentration at a distance of 2.05 μm ahead of the crack tip can reach 1.5% for a bulk concentration of 10 appm. Assuming then that the surface energy can be reduced by a factor of three, the fatigue threshold is correspondingly lowered to about half its value in an inert environment and when no internal hydrogen is present.

Fatigue crack growth thresholds in an external hydrogen environment are also expected to be lowered by chemisorption. For the experiments carried out by Ritchie and Suresh[36,42] in a hydrogen atmosphere, the equilibrium solubility is estimated[37] to be about 0.02 appm. This corresponds at room temperature to a surface coverage which reduces the surface energy by about 0.95 J/m^2. In order to obtain the surface energy of α-Fe in an inert environment, the surface energy and its temperature dependence for δ-Fe[43] is extrapolated back to room temperature. This value so obtained is γ_o = 3.24 J/m^2, so that γ = 2.29 J/m^2 for the hydrogen environment. Hence, the ratio of the fatigue threshold values

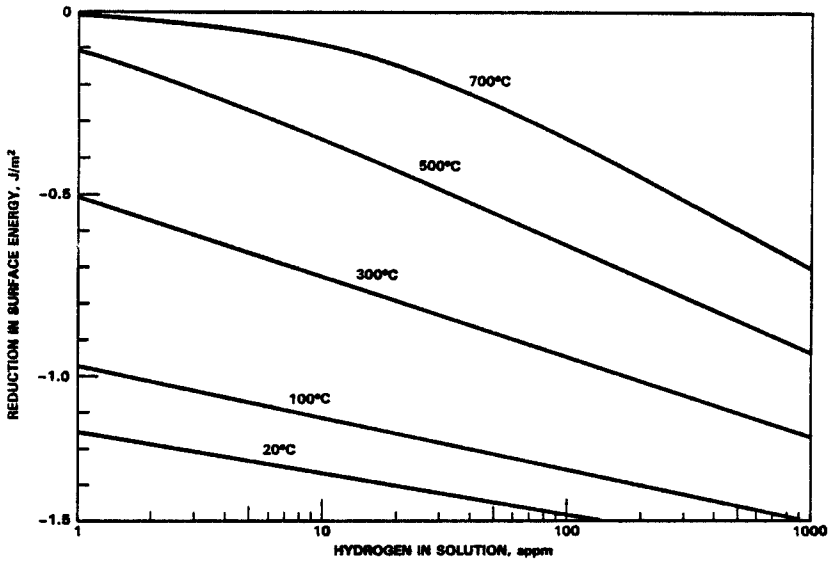

FIGURE 5
Reduction in surface energy versus hydrogen concentration for α - Fe.

in the hydrogen and in the inert environment is expected to be equal to $(\gamma/\gamma_0)^{1/2} = 0.84$. This compares favorably to the measured ratio for the fatigue threshold values of 2-1/4Cr-1Mo steel in hydrogen and helium which is[42] equal to 5.25/6.15 = 0.85.

5. SUMMARY

Models for crack growth processes in austenitic and ferritic stainless steels were evaluated. The effect of impurity segregation on the intergranular K_{IC} of HT-9 was assessed with a model by Gerberich and it was concluded that moderate radiation induced yield strength and/or segregation increases would cause intergranular fracture of HT-9. The effect of impurity segregation, yield strength increases and hydrogen on the intergranular fracture threshold K_{TH} of HT-9 was evaluated with a model by Gerberich. Again, moderate radiation induced yield strength and/or segregation increases caused large decreases in K_{TH}. The effect of radiation induced phosphorus segregation on the IGSCC of 316SS was evaluated using segregation versus fluence data and a stress corrosion model by Parkins. It was estimated that the intergranular crack growth rate of 316SS increased by a factor of 8 after a fluence of 100 dpa. Also, it appears that hydrogen in either external or internal form affects the fatigue threshold by reducing the surface energy relative to its value in an inert environment. However, when compared to threshold values in air, the oxide formation can promote crack closure and thereby increase the fatigue threshold value for R-ratios below a critical value. The latter depends on the oxide layer thickness and the amount of reversed plasticity at the crack tip.

ACKNOWLEDGMENTS

The support of the Office of Fusion Energy by U.S. DOE in part for this work (RHJ) under contract DE-AC06-76RLO 1830 is gratefully acknowledged. This work was also supported in part

(WGW) by the Electric Power Research Institute under contract RP1597-2 with the Univ. of Wisconsin.

REFERENCES

1. J. Kameda and C.J. McMahon, Jr., Metal. Trans. A. 12A (1981) 31.
2. M. Guttman, Mechanics and Physics of Surfaces.
3. M.P. Seah, Surface Science 53 (1975) 168.
4. C.L. White, R.A. Padgett, and R.W. Swindeman, Scripta Met. 15 (1981) 777.
5. J.L. Brimhall, D.R. Baer, and R.H. Jones, J. of Nucl. Mater. 17 (1983) 218.
6. W.W. Gerberich and A.G. Wright, in: Proceedings of the Second International Conference on Environmental Degradation of Engineering Materials, eds. M.R. Louthan, Jr., R.P. McNitt and R.D. Sisson Jr., (Virginia Polytechnic Institute, Blackburg, VA, 1981) p. 183.
7. R.H. Jones and M.T. Thomas, Damage Analysis and Fundamental Studies Quarterly Report for period ending March 31, 1983, DOE/ER-0046/13, Vol. 1, p. 77.
8. F.A. Smidt, Jr., J.R. Hawthorne and V. Provenzano, in: Proceedings of the Tenth International Symposium on Effects of Radiation on Materials, ASTM STP 725, eds. D. Kramer, H.R. Brager and J.S. Perrin, (1980) p. 269.
9. J.R. Hawthorne, Alloy Development for Irradiation Performance Semi-annual Report for period ending March 31, 1982, DOE/ER-0045/8, p. 336.
10. R.H. Jones, S.M. Bruemmer, M.T. Thomas, and D.R. Baer, Met. Trans. A. 13A (1982) 241.
11. J.M. Hyzak and W.M. Garrison, Alloy Development for Irradiation Performance Semi-annual Report for period ending March 31, 1982, DOE/ER-0045/8, (1982) 461.
12. K. Yoshino and C.J. McMahon, Jr., Met. Trans. 5 (1974) 363.
13. C.L. Briant, H.C. Feng, and C.J. McMahon, Jr., Met. Trans. A. 9A (1978) 625.
14. R. Viswanathan and S.J. Hudak, Jr., Met. Trans. A. 8A (1977) 1633.
15. T. Inoue, K. Yamamoto and M. Nagumo, Hydrogen effects in metals, eds. I.M. Bernstein and A.W. Thomson, TMS-AIME (1980) p. 777.
16. C.L. Briant, H.C. Feng, and C.J. McMahon, Jr., Met. Trans. A. 9A (1978) 625.
17. J.C.M. Li, R. Oriani and L.S. Darken, Z. Phys. Chem. 49 (1966) 271.
18. F.P. Ford, Corrosion-fatigue crack propagation, in: Proceedings of the 27th Sagamore Army Materials Conference (Bolton Landing, New York, 1980).
19. D.A. Vermilyea, Stress corrosion cracking and hydrogen embrittlement of iron base alloys, eds. R.W. Staehle, J. Hochmann, R.D. McCright and J.E. Slater, NACE-5, (1973) p. 208.
20. R.N. Parkins, ibid. 601.
21. C.L. Briant, Corrosion 36 (1980) 497.
22. S.M. Bruemmer, R.H. Jones, M.T. Thomas and D.R. Baer, 'in print'.
23. R.H. Jones, S.M. Bruemmer, M.J. Danielson, M.T. Thomas and D.R. Baer, in: Proceedings of localized crack chemistry and mechanics in environment assisted cracking, Fall 1983 TMS-AIME Meeting (Philadelphia, PA, 1983).
24. M. Guttmann, Ph. Dumoulin, N. Tan-Tai and P. Fontaine, Corrosion 37 (1981) 417.
25. P. Marcus, J. Oudar and I. Olefjord, Matl. Sci. and Engr. 42 (1980) 191.
26. A.P. Gulyaev and V.M. Chulkova, Prot. Met. USSR 12 (1970) 259.
27. R.P. Wei and G.W. Simmons, Int. J. Fracture 17 (1981) 235-247.
28. R.O. Ritchie, Inter. Metals Reviews 5,6 Review 245 (1979) 205-230.
29. E. Tschegg and S. Stanzl, Acta Met. 29 (1981) 33-40.
30. S. Stanzl and E. Tschegg, Acta Met. 29 (1981) 21-32.
31. A.T. Stewart, Eng. Fract. Mech. 13 (1980) 463-478.
32. L.K.L. Tu and B.B. Seth, J. Testing and Evaluation 6 (1978) 66-74.
33. S. Purushothaman and J.K. Tien, Matl. Science and Engr. 34 (1978) 241-246.
34. J.C. Radon, Int. J. Fatigue 4 (1982) 161-166.
35. J.C. Radon, Int. J. Fatigue 4 (1982) 225-232.
36. S. Suresh, G.F. Zamiski, and R.O. Ritchie, Fatigue crack propagation behavior of 2-1/4Cr-1Mo steels for thick-wall pressure vessels, ASTM STP 755 (1982) 49-67.
37. J.R.G. Da Silva and R.B. McLellan, J. Less-Common Metals 50 (1976) 1-5.
38. S.W. Stafford and R.B. McLellan, Acta Met. 22 (1974) 1463-1468.
39. K. Christmann, Hydrogen adsorption on metal surfaces, in: Atomistics of Fracture, eds. R.M. Latanision and J.R. Pickens (Plenum Press, New York, 1983) pp. 363-386.
40. G. Bernard and C.H.P. Lupis, Surface Science 42 (1974) 61-85.
41. J.P. Hirth and B. Carnahan, Acta Met. 26 (1978) 1795-1803.
42. R.O. Ritchie and S. Suresh, Effects of crack flank oxide debris and fracture surface roughness on near-threshold corrosion fatigue, in: Atomistics of Fracture, eds. R.M. Latanision and J.R. Pickens (Plenum Press, New York 1983) pp. 835-842.
43. L.E. Murr, Interfacial Phenomena in Metals and Alloys, Addision-Wesley Publ. Comp., Reading, (1975) 124.